

This is a repository copy of *An interplay between molecular pairing, smectic layer spacing, dielectric anisotropy and re-entrant phenomena in  $\omega$ -alkenyloxy cyanobiphenyls*.

White Rose Research Online URL for this paper:  
<https://eprints.whiterose.ac.uk/104726/>

Version: Published Version

---

**Article:**

Mandle, Richard [orcid.org/0000-0001-9816-9661](https://orcid.org/0000-0001-9816-9661) and Goodby, John William (2016) An interplay between molecular pairing, smectic layer spacing, dielectric anisotropy and re-entrant phenomena in  $\omega$ -alkenyloxy cyanobiphenyls. LIQUID CRYSTALS. pp. 1-11. ISSN 1366-5855

<https://doi.org/10.1080/02678292.2016.1227484>

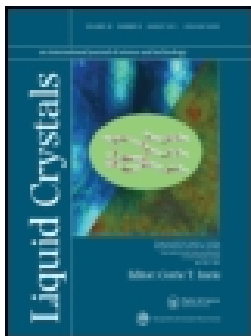
---

**Reuse**

This article is distributed under the terms of the Creative Commons Attribution (CC BY) licence. This licence allows you to distribute, remix, tweak, and build upon the work, even commercially, as long as you credit the authors for the original work. More information and the full terms of the licence here:  
<https://creativecommons.org/licenses/>

**Takedown**

If you consider content in White Rose Research Online to be in breach of UK law, please notify us by emailing [eprints@whiterose.ac.uk](mailto:eprints@whiterose.ac.uk) including the URL of the record and the reason for the withdrawal request.



## An interplay between molecular pairing, smectic layer spacing, dielectric anisotropy and re-entrant phenomena in $\omega$ -alkenyloxy cyanobiphenyls

Richard J. Mandle & John W. Goodby

To cite this article: Richard J. Mandle & John W. Goodby (2016): An interplay between molecular pairing, smectic layer spacing, dielectric anisotropy and re-entrant phenomena in  $\omega$ -alkenyloxy cyanobiphenyls, *Liquid Crystals*, DOI: [10.1080/02678292.2016.1227484](https://doi.org/10.1080/02678292.2016.1227484)

To link to this article: <http://dx.doi.org/10.1080/02678292.2016.1227484>



© 2016 The Author(s). Published by Informa UK Limited, trading as Taylor & Francis Group.



[View supplementary material](#)



Published online: 31 Aug 2016.



[Submit your article to this journal](#)



Article views: 59



[View related articles](#)



[View Crossmark data](#)

## An interplay between molecular pairing, smectic layer spacing, dielectric anisotropy and re-entrant phenomena in $\omega$ -alkenyloxy cyanobiphenyls

Richard J. Mandle  and John W. Goodby

Department of Chemistry, University of York, York, UK

### ABSTRACT

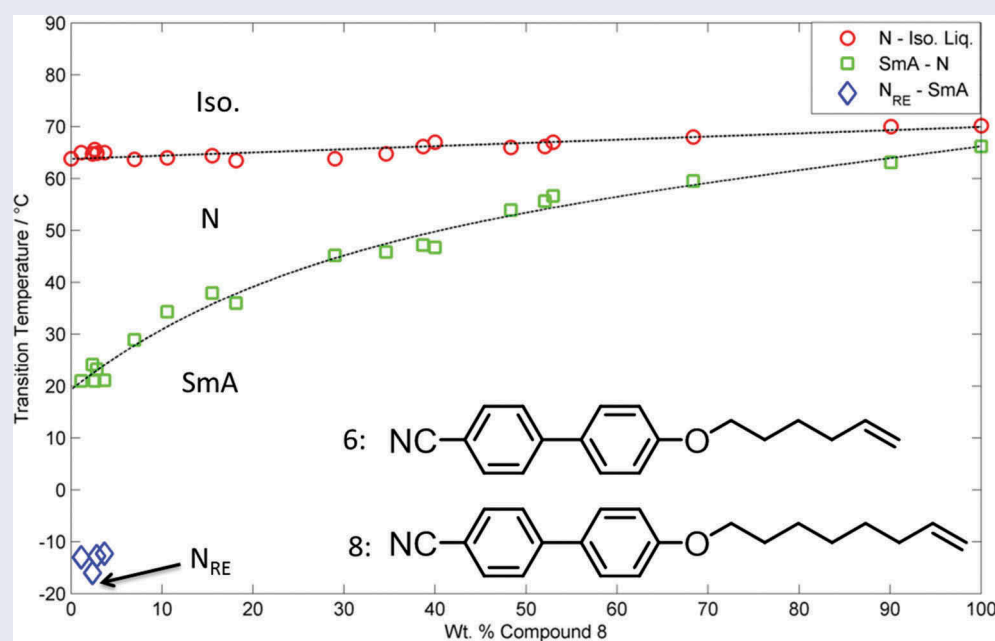
In this article, we report on the liquid-crystalline properties of the 4- $\omega$ -alkenyloxy-4'-cyanobiphenyl series of compounds up to a total aliphatic chain length of eleven. When compared to the analogous fully saturated compounds, we find that the smectic layer spacing is significantly larger for the alkene-terminated materials; conversely the dielectric anisotropy in the nematic phase was found to be significantly smaller. The ability to manipulate bulk properties of nematic and smectic mesophases may have future relevance for display applications.

### ARTICLE HISTORY

Received 18 July 2016  
Accepted 18 August 2016

### KEYWORDS

SAXS; Dielectric; reentrant; liquid crystal




### Introduction

The elucidation of structure–property relationships for mesogenic materials continues to be an important avenue in applied liquid crystal research [1–3]. Knowing the likely impact of the introduction of various functional groups on both bulk properties and mesomorphism underpins the success of engineering of soft materials [3]. For example, the introduction of polar groups has been used for decades to affect changes in the dielectric anisotropy of the resulting liquid crystals [4–8]. Changes in the molecular structure can also be used to entirely alter the mesomorphism of a material, a point illustrated

by considering the behaviour of 8OCB (4-octyloxy-4'-cyanobiphenyl) and its perfluoroalkoxy analogue (4-(1,1,2,2,3,3,4,4,5,5,6,6,7,7,8,8,8-heptafluorooxyloxy)-4'-cyanobiphenyl); 8OCB exhibits a nematic and a smectic A<sub>D</sub> mesophase, whereas the analogous perfluoroalkoxy material exhibits only a smectic A phase [9]. In this example, the lamellar SmA<sub>D</sub> phase is stabilised by nanosegregation which results from the chemical immiscibility of hydrocarbon and fluorocarbon subunits.

Recently, there has been renewed interest in electro-optic devices using the smectic A phase, including dye doped guest–host systems [10–26]. Smectic A devices

**CONTACT** Richard J. Mandle  richard.mandle@york.ac.uk  Department of Chemistry, University of York, York YO10 5DD, UK

 Supplemental data for this article can be accessed [here](#).

© 2016 The Author(s). Published by Informa UK Limited, trading as Taylor & Francis Group.

This is an Open Access article distributed under the terms of the Creative Commons Attribution License (<http://creativecommons.org/licenses/by/4.0/>), which permits unrestricted use, distribution, and reproduction in any medium, provided the original work is properly cited.

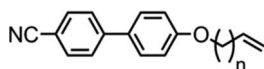


**Figure 1.** General chemical structure of the 4-( $\omega$ -Alkenyloxy)-4'-cyanobiphenyls.

have been stymied by the lack of good host materials that can operate at low voltages, and this has stimulated interest in finding structure–property relationships that can be used to promote the smectic A phase. The stabilisation of the smectic A phase by terminal halogen atoms [27,28] has been reported, however, this behaviour is not exhibited by halo-terminated alkoxy-cyanobiphenyls [29]. A number of bulky terminal groups such as siloxanes [15–17], carbosilanes [30–32], phenoxy [33] and *tert* butyl [32,34] have been reported in the context of materials for electrooptic devices utilising the smectic A phase.

Perhaps due to their utility as chemical intermediates, the properties and mesomorphic behaviour of materials bearing terminal alkenes is often overlooked, or not reported. To our knowledge there has not been a detailed and systematic study on the behaviour of the 4-alkenyloxy-4'-cyanobiphenyl materials, shown in Figure 1, despite many of these compounds being reported previously as chemical precursors to silane and siloxane terminated materials [32].

## Experimental

The liquid crystalline behaviour of the 4-( $\omega$ -alkenyloxy)-4'-cyanobiphenyls was studied using polarised optical microscopy (POM), differential scanning calorimetry (DSC), small angle X-ray scattering (SAXS) and electrooptics, and we compare their results with those of the analogous nOCB series (see Table 1).

The 4- $\omega$ -alkenyloxy-4'-cyanobiphenyls were prepared by the Williamson etherification of 4-hydroxy-4'-cyanobiphenyl with bromoalkenes with potassium carbonate and sodium iodide in acetone. Full

**Table 1.** The transition temperatures ( $^{\circ}\text{C}$ ) of the nOCB series of materials. [35–37].

	$n =$	Cr	$\text{SmA}_D$	N	Iso
3OCB	3	● 44.9	-	(● 40.0)	●
4OCB	4	● 78.0	-	(● 75.5)	●
5OCB	5	● 48.0	-	● 68.0	●
6OCB	6	● 57.0	-	● 75.5	●
7OCB	7	● 54.0	-	● 74.0	●
8OCB	8	● 54.5	● 67.2	● 81.0	●
9OCB	9	● 61.3	● 77.9	● 80.0	●
10OCB	10	● 59.5	● 83.9	-	●
11OCB	11	● 71.5	● 87.5	-	●

experimental details, including synthetic procedures and chemical characterisation, are provided in the accompanying supplemental data to this article. Small angle X-ray scattering was performed on a Bruker D8 Discover using copper K alpha radiation ( $\lambda = 0.1506 \text{ nm}$ ) and a Bruker VANTEC 500 area detector (2048x2048 pixels). The instrument was equipped with a bored graphite rod furnace allowing control of the sample temperature. Alignment was achieved via a pair of 1 T magnets oriented perpendicular to the incident beam, giving a field of approximately 0.6 T at the sample. An INSTEC ALCT property tester was used to obtain values of capacitance as a function of voltage for materials confined in  $3 \mu\text{m}$  cells with planar alignment and ITO electrodes (area  $2.5 \text{ mm}^2$ ). The resulting CV curve was used to determine dielectric anisotropy as described in the supplemental data. Geometry optimisations were performed in Gaussian G09 revision E.01 at the levels of theory described in the text [38].

## Results and discussion

The transition temperatures of compounds 1–9 (presented in Table 2) were determined by a combination of polarised optical microscopy (POM) and differential scanning calorimetry (DSC), with associated enthalpies and entropies of transition measured by DSC. The assignment of smectic mesophases as being of the sub-type smectic  $\text{A}_D$  (i.e. intercalated) was assisted by small angle X-ray scattering.

The transition temperatures for compounds 1–9 were found to be in close agreement with literature values,

**Table 2.** Transition temperatures ( $^{\circ}\text{C}$ ) and associated enthalpies of transition ( $\text{kJ mol}^{-1}$ ) for compounds 1–9.

No	$n$	Cr	$\text{SmA}_D$	N	Iso
1	1	● 80.2 [30.6]	-	-	● 80.7 [1.2]
2	2	● 65.9 [25.7]	-	-	(● 36.3) [0.3]
3	3	● 88.5 [28.4]	-	-	(● 71.5) [0.7]
4	4	● 33.7 [15.6]	-	-	● 52.6 [0.3]
5	5	● 50.4 [30.5]	-	-	● 70.6 [1.4]
6	6	● 36.7 [25.6]	-	-	● 63.8 [0.5]
7	7	● 46.5 [37.6]	-	-	● 73.9 [1.2]
8	8	● 46.2 [32.7]	● 66.2	● 71.4	● 70.2 [0.7]
9	9	● 57.5 [46.7]	● 71.4	● 76.0	● 76.0 [0.4]

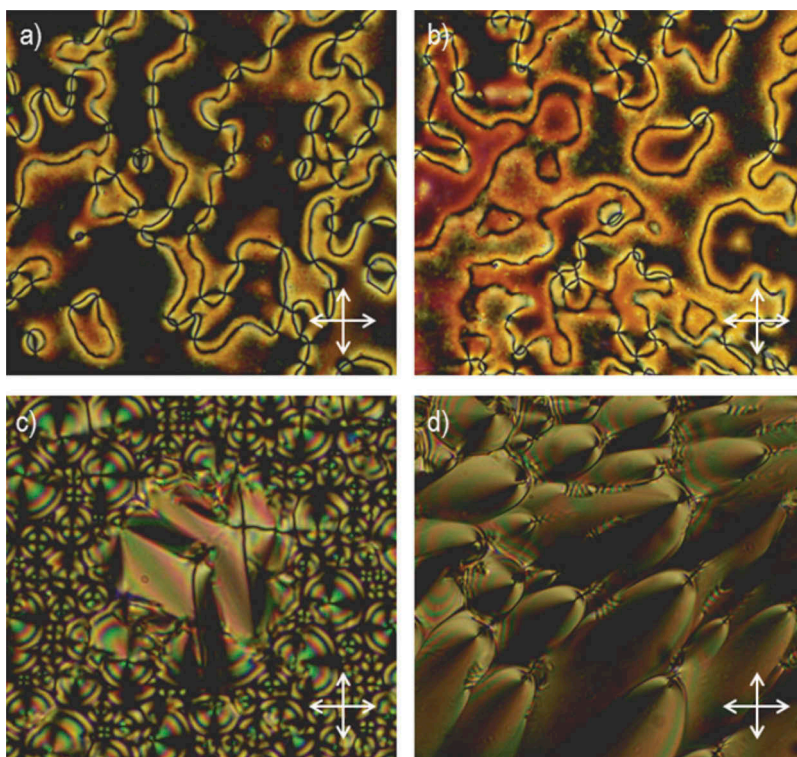


**Figure 2.** (colour online) Photomicrographs (x100) of the *schlieren* texture of the nematic phase of compound **9** at 70.0°C (a and b), a focal-conic defect in the smectic A phase of compound **8** at 66.1°C (c) and numerous parabolic defects in the smectic A phase of compound **9** at 74.8°C (d).

with marginally higher melting and clearing points in several cases [39,40]. With the exception of compounds **1** and **3** the 4- $\omega$ -alkenyloxy-4'-cyanobiphenyls possess both lower melting points and lower nematic to isotropic transition temperatures than the analogous nOCB materials (Table 1). Photomicrographs of the nematic and smectic A phases exhibited by compounds **8** and **9** are given in Figure 2. The nematic phase exhibits a classical *schlieren* texture, whereas the smectic A phase exhibits both the focal-conic and parabolic defects

The enthalpies and entropies associated with the nematic to isotropic transition, plotted in Figure 3, appear to reach a maximum for compounds **5** and **7** before falling again with further increasing chain length. Additionally there is a pronounced odd-even effect, with the magnitude of the associated enthalpies and entropies displaying a dependence on the parity of the 4- $\omega$ -alkenyloxy chain.

The even parity homologues show a smooth increase in the values of the enthalpies and entropies,

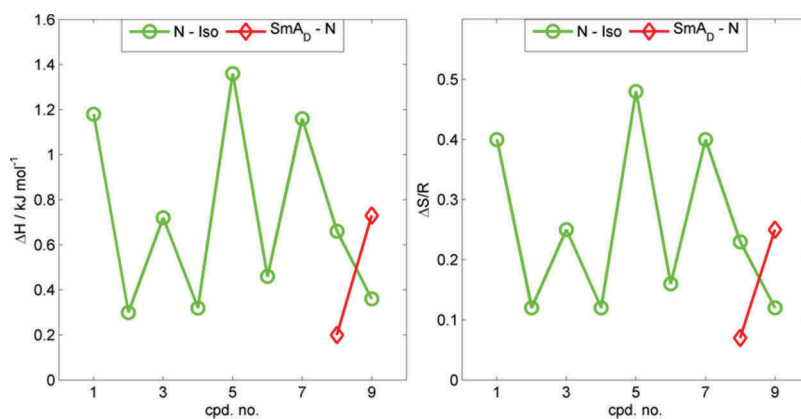


**Figure 3.** (colour online) Plots of associated enthalpies of transition (left,  $\text{kJ mol}^{-1}$ ) and associated dimensionless entropies of transition (right,  $\Delta S/R$ ) for compounds 1–9.

whereas the odd members tend to show more erratic behaviour. This may be related to the orientation of the double bond being closer to the long axes of molecules for even parity, whereas for the odd parity the double bond is oriented off-axis irrespective of the ratio of the *gauche* to *trans* conformations of the methylene chain. To probe this the dipole moment of compounds 1–9 was calculated at the B3LYP/6-31G(d) level of DFT on geometry optimised at the same level of theory. There is an odd–even effect in the dipole moments; however, as the alkene is much less polar than the nitrile group the effect is subtle. The dipole angle – defined here as the angle between the dipole-vector and the mass inertia axis of the molecule – also exhibits a dependence on the parity of the methylene chain (Figure 4).

Both 8OCB and 9OCB exhibit nematic and smectic  $A_D$  phases, whereas the corresponding 4- $\omega$ -alkenyloxy-4'-cyanobiphenyls 6 and 7 only exhibit a nematic mesophase. The assignment of the smectic A phase exhibited by compounds 8 and 9 as the subtype  $A_D$  was made based on SAXS data (representative

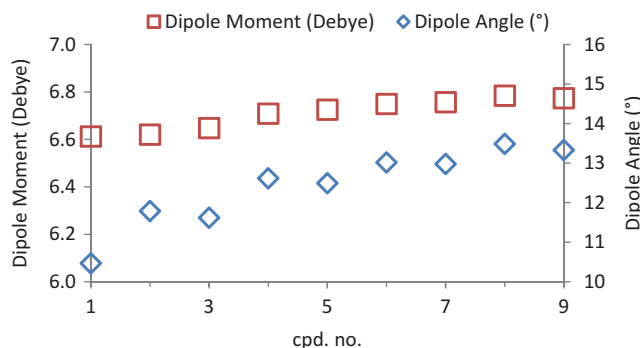


**Figure 4.** (colour online) Plot of molecular dipole moments (calculated at the B3LYP/6-31G(d) level of DFT) and the angle made between the dipole vector and the long-axis of the mesogenic unit.

examples are given in Figure 5); the smectic layer spacing for 8 and 9, as well as the analogous 10OCB and 11OCB, was found to be between 1 and 2 molecular lengths (determined from geometry optimised at the B3LYP/6-31G(d) level of DFT) and thus confirming the  $SmA$  phase as this subtype rather than a monolayer ( $SmA_1$ ) or bilayer ( $SmA_2$ ) phase. The higher homologues of the 4- $\omega$ -alkenyloxy-4'-cyanobiphenyls studied in this work (8 and 9) were found to exhibit both nematic and smectic  $A_D$  mesophases, however, the analogous nOCB compounds (10OCB and 11OCB) both exhibit direct isotropic to smectic  $A_D$  phase transitions with the thermal stability of the smectic  $A_D$  phase being significantly higher for the nOCB materials than for their alkene counterparts. We can therefore state that the incorporation of an alkene at the terminal position of the alkoxy chain of the nOCB materials confers a reduction in clearing points (relative to the saturated parent material), however, the liquid-crystalline state is not entirely suppressed.

Small angle X-ray scattering (SAXS) was used to measure the smectic layer spacing of compounds 8 and 9 along with their saturated analogues (10OCB and 11OCB) as a function of reduced temperature. The molecular lengths of 8, 9, 10OCB and 11OCB were determined from geometry optimised at the B3LYP/6-31G(d) level of theory; using these values in conjunction with measured layer spacing afforded the  $d/l$  ratios plotted in Figure 6.

For 10OCB and 11OCB the smectic layer spacing was found to increase marginally with reduced temperature, however, for compounds 8 and 9 the opposite is true, with the layer spacing (and thus the  $d/l$  ratio) decreasing with reduced temperature. However, for all four compounds the deviation from the mean value was small. Tabulated maxima, minima and mean values of the  $d/l$  ratios along with values at selected reduced temperatures ( $T_{[SmA-N]} - T = 5, 10, 15, 20$  and

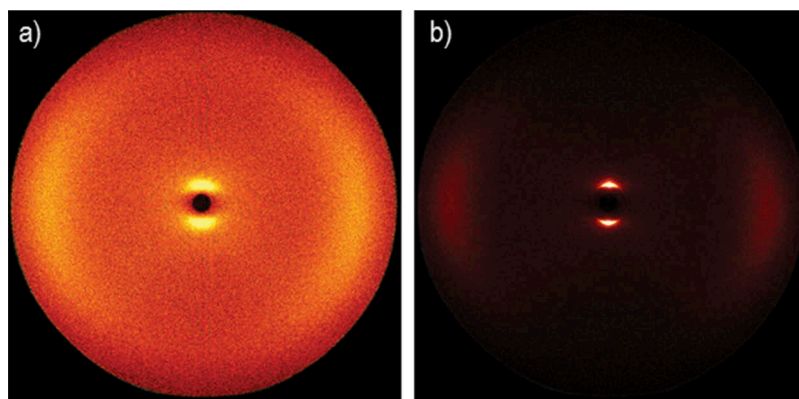


**Figure 5.** (colour online) Two dimensional small angle X-ray scattering patterns obtained for compound 8 in the nematic phase at 69°C (a) and in the smectic  $A_D$  phase at 46°C (b).

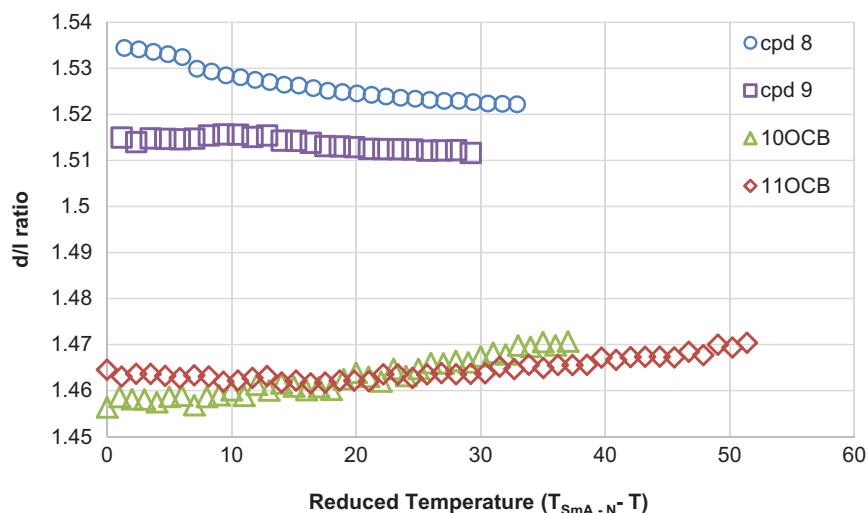


**Figure 6.** (colour online) Plot of the  $d/l$  ratio (see text) vs reduced temperature ( $T_{[SmA-N]} - T$ ) for compounds **8** and **9**, with data for 10OCB and 11OCB for comparison.

25) are given in Table 3. It is interesting to note that although the smectic layer spacings do not exhibit a temperature dependence to the same extent as reported for the 4-undecyloxy-4'-cyanobiphenyls substituted with 'bulky' terminal groups [32], the layer spacing for the alkene terminated materials **8** and **9** is significantly different to that of the analogous saturated nOCB materials. We must add that the pronounced difference in layer spacing between **8/9** and 10OCB/11OCB may be a consequence of differences in the orientational order parameter. Compounds **8** and **9** provide further examples of the ability of terminal groups, in this case alkenes, to manipulate the smectic A layer spacing [30–32].

Initially we assumed that strength of the dipole-dipole interactions between adjacent cyanobiphenyl molecules that lead to antiparallel correlated species is unaffected by the presence or absence of an alkenyl moiety at the terminus of the aliphatic chain; in this scenario the nitrile-to-nitrile distance for adjacent molecules *within* the smectic layers is unchanged, yet the distance between nitrile groups in *adjacent* layers must be larger. In this scenario the layer expansion is caused by the alkenes being 'squeezed' out into the layer interface in a manner similar to that reported for bulky end groups. We cannot at this stage rule

out that the alkene alters the degree antiparallel associations that exist between the cyanobiphenyl group, so as an alternative we speculate that the terminal alkene, through some presently unknown mechanism, leads to an increase the 'aspect ratio' of the antiparallel correlated cyanobiphenyl pair, i.e. the nitrile-to-nitrile distance *within* the smectic layers grows larger, leading to an increase in the smectic layer spacing.

To test these two differing hypotheses experimentally we opted to measure the dielectric anisotropy of compounds **4** and **6**, as well as their saturated analogues 6OCB and 8OCB. These materials were chosen because of their wide nematic phase ranges and convenient operating temperatures. In the Maier–Meier equations the effective dipole moment ( $\mu_{\text{eff}}$ ) is the molecular dipole moment attenuated by the Kirkwood 'g' factor ( $\mu_{\text{eff}}^2 = g\mu_{\text{mol}}^2$ ) which describes the degree of parallel/antiparallel correlation between molecules in a liquid crystal. By using calculated molecular dipole moments and polarisabilities the Kirkwood factor was varied so the calculated dielectric anisotropy from the Maier–Meier equation (see Equations 1–3 below and the ESI for a more detailed discussion) matches the experimental value, giving an empirical value for the degree of antiparallel (or indeed, parallel) molecular correlations that exist in

**Table 3.** Maximum, minimum and mean values of the  $d/l$  ratio along with standard deviation from mean (SD), values at reduced temperatures of 5, 10, 15, 20 and 25. Values of the  $d/l$  ratios were obtained using  $SmA_D$  layer spacings measured by SAXS and molecule lengths obtained at the B3LYP/6-31G(d) level of DFT for compounds **8**, **9**, 10OCB and 11OCB.

No.	Max $d/l$	Min $d/l$	Mean $d/l$	SD	$d/l$ ( $T_R = 5$ )	$d/l$ ( $T_R = 10$ )	$d/l$ ( $T_R = 15$ )	$d/l$ ( $T_R = 20$ )	$d/l$ ( $T_R = 25$ )
<b>8</b>	1.545	1.520	1.527	0.0055	1.533	1.528	1.526	1.524	1.523
<b>9</b>	1.516	1.512	1.514	0.0013	1.515	1.515	1.514	1.513	1.512
10OCB	1.470	1.462	1.464	0.0023	1.463	1.462	1.462	1.463	1.464
11OCB	1.471	1.455	1.462	0.0044	1.459	1.460	1.461	1.464	1.465

the bulk liquid crystal phase [41–47], and thereby allowing us to test our two hypotheses.

$$\epsilon_{\parallel} = 1 + \frac{NFh}{\epsilon_0} \left\{ \bar{\alpha} - \frac{2}{3} \Delta\alpha S + \frac{F\mu_{eff}^2}{3k_B T} [1 - (1 - 3\cos^2\beta)S] \right\} \quad (1)$$

$$\epsilon_{\perp} = 1 + \frac{NFh}{\epsilon_0} \left\{ \bar{\alpha} - \frac{1}{3} \Delta\alpha S + \frac{F\mu_{eff}^2}{3k_B T} \left[ 1 + \frac{1}{2} (1 - 3\cos^2\beta) S \right] \right\} \quad (2)$$

$$\Delta\epsilon = \epsilon_{\parallel} - \epsilon_{\perp} = \frac{NFh}{\epsilon_0} \left\{ \Delta\alpha - \frac{F\mu_{eff}^2}{2k_B T} (1 - (3\cos^2\beta)) \right\} S \quad (3)$$

Thus, plots of capacitance as a function of voltage (triangular waveform, 1 kHz) were used to obtain the dielectric anisotropy as described in the ESI, with a representative plot of capacitance as a function of voltage shown in Figure 7. Values for the dielectric anisotropy were collected as a function of reduced temperature, with values approaching saturation at

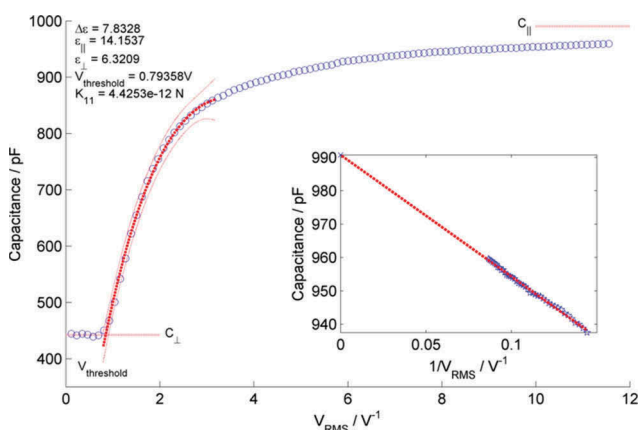
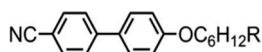


**Figure 7.** (colour online) Plot of capacitance (pF) as a function of RMS voltage (V) obtained for compound **6** using a triangular waveform at a temperature of 35°C, with an inset showing a plot of capacitance as a function of 1/V with a linear fit used to determine  $C_{\parallel}$  and thus  $\epsilon_{\parallel}$ . Blue circles correspond to experimental data, whereas the dashed red lines correspond to fits used to obtain  $C_{\parallel}$  and  $V_{\text{threshold}}$ .

8.2 and 7.8 respectively at a reduced temperature of 25°C for both compounds **4** and **6**; these values are significantly lower than those obtained for 6OCB and 8OCB by us previously ( $\Delta\epsilon = 10.9$  for both) [29,47]. Qualitatively, this result is indicative of the Kirkwood factor being smaller for alkene terminated materials than their saturated analogues, i.e. there is a greater degree of antiparallel pairing. Using dipole and polarisability data (B3LYP/6-31G(d) level of theory) solutions to the Maier–Meier equations were found for a reasonable range of order parameters ( $S = 0.4, 0.5$  and  $0.6$ ) yielding the Kirkwood factor for each case (Table 4). As noted by Kaszynski *et al.*, systematic errors that result from quantum chemical calculations are included in the empirical Kirkwood factor, and thus comparisons of results obtained for closely related compounds or materials examined in the same medium are still valid, provided calculations are performed at the same level of theory [46].

As expected for the two closely related molecular structures the dipole moments and polarisabilities of 8OCB and **6** are almost identical (tabulated data is presented in ESI), hence, the large difference in the dielectric anisotropy of these two materials is surprising. By adjusting both the Kirkwood factor ( $g$ ) and order parameter ( $S$ ) used when obtaining solutions to the Maier–Meier equation it is possible to match the calculated values of dielectric anisotropy with those measured experimentally. As the order parameter is not known, a range of reasonable values were used (0.4, 0.5 and 0.6), with back-calculation giving the Kirkwood factors shown in Table 4. Determination of the order parameter from dielectric permittivities (see ESI for details) yielded values of 0.44, 0.41 and 0.48 for **4**, **6** and 6OCB respectively at reduced temperatures of 25°C, whereas for 8OCB a value of 0.45 was obtained prior to the N-SmA phase transition (reduced temperature of approximately 13°C). The difference in experimentally measured  $\Delta\epsilon$  between both pairs (i.e. **4**/6OCB and **6**/8OCB) means that, for a given value of the order parameter, the resulting Kirkwood factor for the alkene-terminated material is smaller than that of the analogous nOCB. In other words, there is a greater

**Table 4.** Transition temperatures (°C), associated enthalpies of transition [ $\text{kJ mol}^{-1}$ ], dielectric anisotropies ( $\Delta\epsilon$ ) and calculated Kirkwood factors ( $g_5$  at order parameters [ $S$ ] 0.4, 0.5 and 0.6 respectively) for 6OCB, 8OCB [29,47] compounds **4** and **6** (this work).



R =	No.	Cr	SmA	N	Iso	$\Delta\epsilon$	$g_{0.4}$	$g_{0.5}$	$g_{0.6}$
H <sub>3</sub> C–CH <sub>2</sub> –	6OCB	•	57.0	-	•	10.9	0.266	0.215	0.178
H <sub>2</sub> C = CH–	<b>4</b>	•	33.7	-	•	8.2	0.221	0.177	0.147
H <sub>3</sub> C–CH <sub>2</sub> –	8OCB	•	54.5	•	•	10.9	0.301	0.242	0.202
H <sub>2</sub> C = CH–	<b>6</b>	•	36.7	-	•	7.8	0.242	0.191	0.159



degree of antiparallel pairing associated with the incorporation of a terminal alkene. A weak interaction between a nitrile and alkene has been reported [48], and this may be the origin of the reduced Kirkwood factor (and thereby the reduction in dielectric anisotropy) in alkene-terminated nOCB compounds.

Reentrant behaviour in liquid crystals, where a 'less' ordered mesophase is obtained on cooling a 'more' ordered mesophase – although more correctly a phase of higher symmetry is obtained on cooling a phase of lower symmetry – is a well-established phenomenon [49,50], and exists in analogy to similar reentrant behaviour observed in other systems [51]. Binary mixtures of 6OCB in 8OCB exhibit the phase sequence N-SmA-N<sub>RE</sub> (where N<sub>RE</sub> is a reentrant nematic phase) when the concentration of 6OCB is in the range of 20–30 wt%. As described by Cladis, the reentrant polymorphism in the 6OCB/8OCB system is a consequence of the formation of antiparallel correlated pairs, the population (relative to unpaired molecules) and lifetime for which increases with decreasing temperature. As the temperature decreases (and the relative population of paired molecules increases) the dipolar forces that stabilise the layered structure break down, leading the material to revert to the nematic phase. The difference in length between an unbound single molecule and a dimer pair is significant; this incommensurability of length scales has been postulated to be the origin of multiple reentrancies (for example the multiple nematic phases of DB<sub>9</sub>ONO<sub>2</sub>) [52,53]. We opted to explore the phase diagram between compounds **6** and **8** on the basis that if, as suggested from dielectric measurements, the presence of a terminal alkene leads to an increase in the degree of antiparallel correlated pairs then such a phase diagram should be expected to exhibit the N-SmA-N<sub>RE</sub> phase sequence.

As shown in Figure 8, the smectic A phase persists over almost the entire concentration range to as low as 1.1 wt% of compound **8**. The clearing point varies almost linearly with concentration; however, the SmA-N transition decays exponentially. A transition from the smectic A phase to a reentrant nematic was observed at low temperature for mixtures with <5 wt% of compound **8**; at the next highest concentration of **8** (7 wt%) the smectic A phase crystallises at around 0°C, whereas for pure **6** the material crystallises at around 25°C from the nematic phase. For the smectic A phase, the *schlieren* texture re-appeared, with the sample becoming noticeably less viscous, despite the temperature of this phase transition being around –15°C. The nematic and smectic A phases were identified by polarised optical microscopy based on their

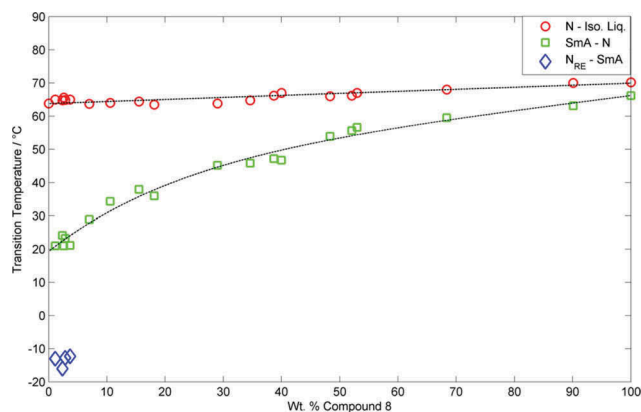


**Figure 8.** (colour online) Gibbs phase diagram for binary mixtures (wt %) of compounds **6** and **8**. Melting points are omitted for clarity. Dashed lines correspond to linear fit of and a double exponential fit of SmA-N as a function of composition.

characteristic defect textures as described earlier in the text. In the case of the reentrant nematic phase, the optical textures are identical to those of the nematic; homeotropically oriented regions in the smectic A phase retain this alignment in the reentrant nematic phase, whereas the focal-conic defects yield a classical *schlieren* texture confirming that the lower temperature phase is not smectic C. At present, experimental limitations prevent the measurement of the smectic layer spacing below ambient temperature (~ 20°C) by SAXS, however, this would potentially afford quantitative information about the degree of pairing; for example in the 6OCB/8OCB system it is known that the degree of pairing is inversely proportional to temperature and as the level of pairing saturates the transition to the reentrant nematic phase occurs. As the reentrant nematic occurs at around 50°C lower for the **6/8** phase diagram ( $T_{\text{SmA-Nre}} \sim -15^\circ\text{C}$ ) than for 6OCB/8OCB ( $T_{\text{SmA-Nre}} \sim 35^\circ\text{C}$ ) this indicates that, qualitatively, the degree of pairing for the alkene-terminated materials does not saturate until a much lower temperature than for the 4-alkoxy-4'-cyanobiphenyls. This is not to say that the degree of pairing is actually less in the alkene terminated materials, but rather it may simply saturate at some higher value. If the reentrant nematic phase observed for binary mixtures of both 6OCB/8OCB and **6/8** is considered to be a product of the incommensurability between the length of free molecule and the 'dimer' type species, then the increased degree of pairing in the alkene-terminated materials would be expected to lead to a more stable smectic A phase through the reduction in the number of free molecules which destabilise the smectic A phase and lead to the nematic.

## Conclusions

Despite the similarity of their chemical structures, the properties of the condensed phases exhibited by the alkenyloxy- and alkoxy-cyanobiphenyls differ significantly. In the smectic A phase, the  $d/l$  ratio (the layer spacing divided by the molecular length obtained at the DFT(B3LYP)/6-31G(d) level) was found to be significantly larger for alkene terminated materials than the analogous nOCB compounds. The  $d/l$  ratio measured for 10OCB and 11OCB are approximately equivalent at a given reduced temperature, those for the analogous alkene terminated materials (compounds **8** and **9**) exhibit significant differences. This result gives important fundamental information for the underpinning of the design of the molecular architectures of materials for applications in nematic and smectic flat panel displays.

Two main hypotheses were formulated, either the alkenes are expelled to the layer interface in an analogous fashion to that claimed for bulky groups [32], or the alkenes somehow change the nature of the antiparallel associations that exists between adjacent cyanobiphenyl units. To test this, we measured dielectric anisotropy, if this had remained the same then the second hypothesis was null, however, in the nematic phases we observed a sharp reduction in dielectric anisotropy. The fall in  $\Delta\epsilon$  is, we believe, attributable to increase antiparallel pairing of the molecules, i.e. the Kirkwood factor is smaller. This is a counterintuitive result – the alkene is not conjugated to the core and would not be expected to confer any change in dielectric properties. The ability to fine tune the degree of antiparallel correlation that occurs in polar calamitic liquid crystals has the potential to be an important design feature in the synthesis of materials with very large values of dielectric anisotropy, i.e.  $\Delta\epsilon > 50$ , where aggregation effects can become significant [44]. Low concentration binary mixtures of compound **8** (<5 wt%) with compound **6** yield the reentrant phase sequence N-SmA-N<sub>re</sub>.

## Acknowledgements

We would like to thank the Engineering and Physical Sciences Research Council (EPSRC) for support of this work via grant codes [EP/K039660/1 and EP/M020584/1]. Raw data are available upon request from the University of York data catalogue.

## Disclosure statement

No potential conflict of interest was reported by the authors.

## Funding

This work was supported by the Engineering and Physical Sciences Research Council (EPSRC): Grant Numbers [EP/K039660/1 and EP/M020584/1].

## ORCID

Richard J. Mandle  <http://orcid.org/0000-0001-9816-9661>

## References

- Demus D. One hundred years of liquid crystal chemistry - thermotropic liquid crystals with conventional and unconventional structure. *Liq Cryst.* 1989;5:75–110. doi:10.1080/02678298908026353.
- Goodby JW, Gray GW. Molecular structure and the polymorphism of smectic liquid crystals. *J Phys (Paris)*. 1976;37:C3-17- C3-26. doi:10.1051/jphyscol:1976303.
- Goodby JW. The nanoscale engineering of nematic liquid crystals for displays. *Liq Cryst.* 2011;38:1363–1387. doi:10.1080/02678292.2011.614700.
- Reiffenrath V, Krause J, Plach HJ, et al. New liquid-crystalline compounds with negative dielectric anisotropy. *Liq Cryst.* 1989;5:159–170. doi:10.1080/02678298908026359.
- Hird M, Goodby JW, Toyne KJ. Nematic materials with negative dielectric anisotropy of display applications. *Proc SPIE.* 2000;3955:15–23. doi:10.1117/12.379979.
- Gasowska JS, Cowling SJ, Cockett MCR, et al. The influence of an alkenyl terminal group on the mesomorphic behaviour and electro-optic properties of fluorinated terphenyl liquid crystals. *J Mater Chem.* 2009;20:299–307. doi:10.1039/b914260f.
- Kirsch P, Bremer M, Heckmeier M, et al. Liquid crystals based on hypervalent sulfur fluorides: pentafluor-sulfuranyl as a polar terminal group. *Angew Chem Int Ed.* 1999;38:1989–1992. doi:10.1002/(SICI)1521-3773(19990712)38:13/14<1989::AID-ANIE1989>3.0.CO;2-.
- Jankowiak A, Ringstrand B, Janusko A, et al. Liquid crystals with negative dielectric anisotropy: the effect of unsaturation in the terminal chain on thermal and electro-optical properties. *Liq Cryst.* 2013;5:605–615. doi:10.1080/02678292.2013.774064O.
- Jang JY, Park YW. Synthesis and structural studies of smectic C mesogens with terminal perfluoroalkyl chains. *Liq Cryst.* 2013;40:511–515. doi:10.1080/02678292.2012.761356.
- Tani C. Novel electro-optical storage effect in a certain smectic liquid crystal. *Appl Phys Lett.* 1971;19:241–242. doi:10.1063/1.1653902.
- Hareng M, Le Berre S. Defects – applications to display devices thermal relaxation recording device on smectic liquid crystals. *J Phys Coll.* 1976;C3-135–C3-136. doi:10.1051/jphyscol:1976326.
- Coates D, Crossland WA, Morris JH, et al. Electrically induced scattering textures in smectic A phases and their electrical reversal. *J Phys D: Appl Phys.* 1978;11:2025–2034. doi:10.1088/0022-3727/11/14/012.
- Khosla S, Raina KK, Coles HJ. Electrically induced storage effects in smectic A phase of dyed low molar mass

- siloxane liquid crystals. *Curr Appl Phys.* 2003;3:135–140. doi:10.1016/S1567-1739(02)00191-8.
14. Gheorghiu N, West JL, Glushchenko AV, et al. Patterned field induced polymer walls for smectic A bistable flexible displays. *Appl Phys Lett.* 2006;88:263511-1–263511-4. doi:10.1063/1.2218274.
15. Gardiner DJ, Coles HJ. Organosiloxane liquid crystals for fast-switching bistable scattering devices. *J Phys D: Appl Phys.* 2006;39:4948–4955. doi:10.1088/0022-3727/39/23/008.
16. Gardiner DJ, Davenport CJ, Newton J, et al. Electro-optic bistability in organosiloxane bimesogenic liquid crystals. *J Appl Phys.* 2006;99:113517-1–113517-4. doi:10.1063/1.2203391.
17. Gardiner DJ, Coles HJ. Highly anisotropic conductivity in organosiloxane liquid crystals. *J Appl Phys.* 2006;39:4948–4955. doi:10.1063/1.2398081.
18. Chen H-Y, Shao R, Korblova E, et al. A bistable liquid-crystal display mode based on electrically driven smectic A layer reorientation. *Appl Phys Lett.* 2007;91:163506-1–163506-4. doi:10.1063/1.2799742.
19. Chen H-Y, Shao R, Korblova E, et al. Bistable SmA liquid-crystal display driven by a two-direction electric field. *J Soc Info Display.* 2008;16:675–681. doi:10.1889/1.2938869.
20. Gardiner DJ, Morris SM, Coles HJ. High-efficiency multistable switchable glazing using smectic A liquid crystals. *Sol Energ Mat Sol Cells.* 2009;93:301–306. doi:10.1016/j.solmat.2008.10.023.
21. Chen H-Y, Wu J-S. A multistable smectic-A liquid-crystal device with low threshold field. *J Soc Info Display.* 2010;18:415–420. doi:10.1889/JSID18.6.415.
22. Lu Y, Guo J, Wang H, et al. Flexible bistable smectic-A liquid crystal device using photolithography and photo-induced phase separation. *Adv In Cond Mat Phys.* 2012. doi:10.1155/2012/843264.
23. Chen C-H, Zyryanov VY, Lee W. Switching of defect modes in a photonic structure with a tristable smectic-A liquid crystal. *Appl Phys Express.* 2012;5:082003-1–082003-3. doi:10.1155/2012/843264.
24. Lu Y, Wei J, Shi Y, et al. Effects of fabrication condition on the network morphology and electro-optical characteristics of a polymer-dispersed bistable smectic A liquid-crystal device. *Liq Cryst.* 2013;40:581–588. doi:10.1080/02678292.2013.776708.
25. Gardiner DJ, Coles HJ. High-solubility liquid crystal dye guest-host device. *Proc SPIE.* 2007;6587. DOI:10.1117/12.723041
26. Deshmukh RR, Jain AK. The complete morphological, electro-optical and dielectric study of dichroic dye-doped polymer-dispersed liquid crystal. *Liq Cryst.* 2014;41:960–975. doi:10.1080/02678292.2014.896051.
27. Goodby JW, Saez IM, Cowling SJ, et al. Transmission and amplification of information and properties in nanostructured liquid crystals. *Angew Chem Int Ed.* 2008;47:2754–2787. doi:10.1002/anie.200701111.
28. Rupar I, Mulligan KM, Roberts JC, et al. Elucidating the smectic A-promoting effect of halogen end-groups in Calamitic liquid crystals. *J Mater Chem C.* 2013;1:3729–3735. doi:10.1039/C3TC30534A.
29. Davis EJ, Mandle RJ, Russell BK, et al. Liquid-crystalline structure-property relationships in halogen terminated derivatives of cyanobiphenyl. *Liq Cryst.* 2014;41:1635–1645. doi:10.1080/02678292.2014.940505.
30. Schubert CPJ, Bogner A, Porada JH, et al. Design of liquid crystals with ‘de Vries-like’ properties: carbosilane-terminated 5-phenylpyrimidine mesogens suitable for chevron-free FLC formulations. *J Mater Chem C.* 2014;2:4581–4589. doi:10.1039/C4TC00393D.
31. Mulligan KM, Bogner A, Song Q, et al. Design of liquid crystals with ‘de Vries-like’ properties: the effect of carbosilane nanosegregation in 5-phenyl-1,3,4-thiadiazole mesogens. *J Mater Chem C.* 2014;2:8270–8276. doi:10.1039/C4TC01364F.
32. Mandle RJ, Davis EJ, Voll CCA, et al. Self-organisation through size-exclusion in soft materials. *J Mater Chem C.* 2015;3:2380–2388. doi:10.1039/C4TC02991G.
33. Thompson M, Carkner C, Bailer A, et al. Tuning the mesogenic properties of 5-alkoxy-2-(4-alkoxyphenyl) pyrimidine liquid crystals: the effect of a phenoxy end-group in two sterically equivalent series. *Liq Cryst.* 2014;41:1246–1260. doi:10.1080/02678292.2014.913721.
34. Bennani YL, Coner SE, Dinges J, et al. Aminoalkoxybiphenylnitriles as Histamine-3 receptor ligands. *Bioorg Med Chem Lett.* 2002;12:3077–3079. doi:10.1016/S0960-894X(02)00648-0.
35. Mandle RJ, Davis EJ, Sarju JP, et al. Control of free volume through size exclusion in the formation of smectic C phases for display applications. *J Mater Chem C.* 2015;3:4333–4344. doi:10.1039/c5tc00552c.
36. Itahara T, Tamura H. Comparison of liquid crystalline properties of symmetric and nonsymmetric liquid crystal trimers. *Mol Cryst Liq Cryst.* 2007;474:17–27. doi:10.1080/15421400701617749.
37. Mouquino A, Saavedra M, Maiou A, et al. Films based on new methacrylate monomers: synthesis, characterisation and electrooptical properties. *Mol Cryst Liq Cryst.* 2011;542:557–566. doi:10.1080/15421406.2011.570154.
38. Frisch MJ, Trucks GW, Schlegel HB, et al. Gaussian 09, revision E.01. Wallingford (CT): Gaussian; 2009.
39. Zuev VV. 4-allyloxy-4'-cyanobiphenyl. A photoluminescing nematic liquid crystalline compound. *Russian J Gen Chem.* 2006;76:498. doi:10.1134/S1070363206030261.
40. Shepperson KJ, Meyer T, Mehl GH. Polyphilic multi-component dimers with perfluorinated cores. *Mol Cryst Liq Cryst.* 2004;411:185–191. doi:10.1080/15421400490435026.
41. Maier W, Meier G. A simple theory of the dielectric characteristics of homogeneously orientated liquid-crystalline phases of the nematic type. *Z Naturforsch.* 1921;16A:262–267.
42. Onsager L. Electric moments of molecules in liquids. *JACS.* 1932;58:1486–1493. doi:10.1021/ja01299a050.
43. Urban S. Static dielectric properties of nematics. In: Dunmur DA, Fukuda A, Luckhurst GR, editors. *Physical properties of liquid crystals: nematics.* London: IEEE; 2001. p. 267–276.
44. Ringstrand B, Kaszynski P, Januszko A, et al. Polar derivatives of the [closo-1-CB<sub>9</sub>H<sub>10</sub>]<sup>-</sup> cluster as positive Δε additives to nematic hosts. *J Mater Chem.* 2009;19:9204–9212. doi:10.1039/b913701g.
45. Ran Z, Jun H, Zeng-Hui P, et al. Calculating the dielectric anisotropy of nematic liquid crystals: a

- reinvestigation of the Maier-Meier theory. *Chin Phys B*. 2009;18:2885–2892. doi:10.1088/1674-1056/18/7/044.
46. Kaszynski P, Januszko A, Glab KL. Comparative analysis of fluorine-containing mesogenic derivatives of carborane, bicyclo[2.2.2]octane, cyclohexane and benzene using the Maier-Meier theory. *J Phys Chem B*. 2014;118:2238–2248. doi:10.1021/jp411343a.
47. Mandle RJ, Cowling SJ, Sage I, et al. Relationship between molecular association and reentrant phenomena in polar calamitic liquid crystals. *J Phys Chem B*. 2015;119:3273–3280. doi:10.1021/jp512093j.
48. Aliev AE, Arendorf JRT, Pavlakos I, et al. Surfing  $\pi$ -clouds for noncovalent interactions: arenes versus alkenes. *Angew Chem Int Ed*. 2015;54:551–555. doi:10.1002/anie.201409672.
49. Cladis PE. New liquid crystal phase diagram. *Phys Rev Lett*. 1975;35:48–51. doi:10.1103/PhysRevLett.35.48.
50. Cladis PE, Mandle RJ, Goodby JW. Reentrant phase transitions in liquid crystals. In: Goodby JW, Collings PJ, Kato T, et al., editors. *The handbook of liquid crystals*. 2nd ed. Weinheim: Wiley-VCH; 2014.
51. Riblet G, Winzer K. Vanishing of superconductivity below a second transition temperature in  $(\text{La}_{1-x}\text{Ce}_x)\text{Al}_2$  alloys due to the Kondo effect. *Solid State Commun*. 1971;9:1663–1665. doi:10.1016/0038-1098(71)90336-X.
52. Tinh NH, Hardouin F, Desterade C. Trois phénomènes reentrants dans un produit pur mésogène. *J Physique*. 1982;43:1127. doi:10.1051/jphys:019820043070112700.
53. Shashidhar R, Ratna BR, Surendranath V, et al. Experimental studies on a triply reentrant mesogen. *J Physique Lett*. 1985;46:L445–L450. doi:10.1051/jphyslet:019850046010044500.